Mechanism of the Competition between Phenyl Insertion and Ligand Reductive Elimination on a Hindered Platinum(IV) Cyclometalated Complex

Carlos Gallego,[†] Manuel Martínez,*[,†] and Vicent Sixte Safont[‡]

Departament de Química Inorgànica, Universitat de Barcelona, Martí i Franquès 1-11, E-08028 Barcelona, Spain, and Departament de Ciències Experimentals, Universitat Jaume I, Campus del Riu Sec, E-12080 Castelló, Spain

Received September 7, 2006

Careful tuning of the reaction conditions has been proved to be essential for the operation of two disjunctive reaction mechanisms occurring on the ortho-metalated platinum compounds $[Pt^{IV}Br(Ph)_2(C_5CH_4CHN\mathbf{Z})(SMe_2)]$ ($\mathbf{Z}$ = Me, Bzl, $CH_2(2,4,6\text{-}Me_3C_6H_2)$). In dilute solutions, where the already established lability of the SMe_2 ligand favors the existence of the pentacoordinated $\{Pt^{IV}Br(Ph)_2(C_4CH_4CHN\mathbf{Z})\}$ species, the complex evolves to produce the insertion of one of the phenyl ligands into the cyclometalated $Pt^{IV}-C$ bond to yield the complexes $[Pt^{II}Br(C_4CH_3C_6H_4CHN\mathbf{Z})(SMe_2)]$, which contain a seven-membered cyclometalated ring. The process involves the formation of an hydride intermediate, which has been detected via low-temperature proton NMR for $\mathbf{Z}$ = Bzl, prior to the reductive elimination of benzene. In more concentrated solutions, or in the presence of large amounts (200−500 fold) of SMe_2, the existence of pentacoordinated species is reduced to a minimum and a reductive C−C coupling takes place between the metalated imine carbon and one of the phenyl ligands, yielding the coordination complexes $[Pt^{II}Br(Ph)(C_6H_3C_6H_4CHN\mathbf{Z})(SMe_2)]$, which evolve rapidly to *trans*-$[Pt^{II}Br(Ph)(SMe_2)_2]$ and free $C_5H_3C_6H_4CHN\mathbf{Z}$. The validity of the mechanisms proposed has been proved via stoichiometric and reactivity studies carried out under carefully controlled conditions, both on initial Pt^{IV} complex and on the final inserted complex, $[Pt^{II}Br(C_4CH_3C_6H_4CHN\mathbf{Z})(SMe_2)]$. The overall reactivity is rather surprising, given the generally accepted dissociative processes involved in the preliminary steps of reductive elimination reactions on Pt^{IV} complexes. DFT calculations have been carried out in order to check the energetic validity of the proposed disjunctive reaction mechanisms. From the data obtained, it is clear that the formation of the pentacoordinated species $\{Pt^{IV}Br(Ph)_2(C_5CH_4CHN\mathbf{Z})\}$ could effectively lead to the standard C−C reductive coupling, but in our case the existence of the parallel insertion process is highly favored. As a consequence the observed reductive elimination reaction can only occur via the otherwise less favored direct C−C coupling on the octahedral $[Pt^{IV}Br(Ph)_2(C_4CH_4CHN\mathbf{Z})(SMe_2)]$ starting material.

Introduction

The chemistry on octahedral organometallic complexes of Pt(IV) is very often related exclusively to reductive elimination−oxidative addition processes.[1−5] Although substitution reactions are generally linked to such processes, very few studies have been carried out in that field.[6−10] The existence of an intermediate species with a lower coordination number has been repetitively established as crucial for both the oxidative addition and reductive elimination reactions to and from Pt(II) square-planar centers with more than one Pt−C bond.[11−17] Nevertheless, it has been recently demonstrated that the existence of such an intermediate of lower coordination number is not absolutely necessary for these reactions and that the nature of the inert skeleton on the platinum center (namely the nature and rigidity of the donors) plays a crucial role in the process.[18,19] In this respect, we have been involved in the study of the associativity−dissociativity tuning of the substitution reactions of organome-

[†] Universitat de Barcelona.
[‡] Universitat Jaume I.

(1) Canty, A. J.; Rodemann, T. *Inorg. Chem. Commun.* **2003**, *6*, 1382−1384.
(2) Puddephatt, R. J. *Coord. Chem. Rev.* **2001**, *219*−*221*, 157−185.
(3) Rendina, L. M.; Puddephatt, R. J. *Chem. Rev.* **1997**, *97*, 1735−1754.
(4) Crespo, M.; Martínez, M.; de Pablo, E. *J. Chem. Soc., Dalton Trans.* **1997**, 1231−1235.
(5) Crespo, M.; Martínez, M.; Sales, J. *Organometallics* **1992**, *11*, 1288−1295.
(6) Frey, U.; Helm, L.; Merbach, A. E.; Romeo, R. *J. Am. Chem. Soc.* **1989**, *111*, 8161−8165.
(7) Tobe, M. L.; Burgess, J. *Inorganic Reaction Mechanisms*; Longman: Essex, U.K., 1999.
(8) Peloso, A. *Coord. Chem. Rev.* **1973**, *10*, 123−181.
(9) Dixon, N. E.; Lawrance, G. A.; Lay, P. A.; Sargeson, A. M. *Inorg. Chem.* **1984**, *23*, 2940−2947.
(10) Drougge, L.; Elding, L. I. *Inorg. Chim. Acta* **1986**, *121*, 175−183.
(11) Puddephatt, R. J. *Angew. Chem., Int. Ed.* **2002**, *41*, 261−263.
(12) Felk, U.; Zahl, A.; van Eldik, R. *Organometallics* **1999**, *18*, 4156−4164.
(13) Hill, G. S.; Rendina, L. M.; Puddephatt, R. J. *Organometallics* **1995**, *14*, 4966−4968.
(14) Procelewska, J.; Zhal, A.; Liehr, G.; van Eldik, R.; Smythe, N. A.; Williams, B. S.; Goldberg, K. I. *Inorg. Chem.* **2005**, *44*, 7732−7742.
(15) Arthur, K. L.; Wang, Q. L.; Bregel, D. M.; Smythe, N. A.; O'Neil, B. A.; Goldberg, K. I.; Moloy, K. G. *Organometallics* **2005**, *24*, 4624−4628.
(16) Lersch, M.; Tilset, M. *Chem. Rev.* **2005**, *105*, 2471−2526.
(17) Wik, B. J.; Ivanovic-Burmazovic, I.; Tilset, M.; van Eldik, R. *Inorg. Chem.* **2006**, *45*, 3613−3621.
(18) Crumpton, D. M.; Goldberg, K. I. *J. Am. Chem. Soc.* **2003**, *125*, 9442−9456.
(19) West, N. W.; Reinartz, S.; White, P. S.; Templenton, J. L. *J. Am. Chem. Soc.* **2006**, *128*, 2059−2066.

10.1021/om060818e CCC: $37.00 © 2007 American Chemical Society
Publication on Web 12/23/2006

Scheme 1

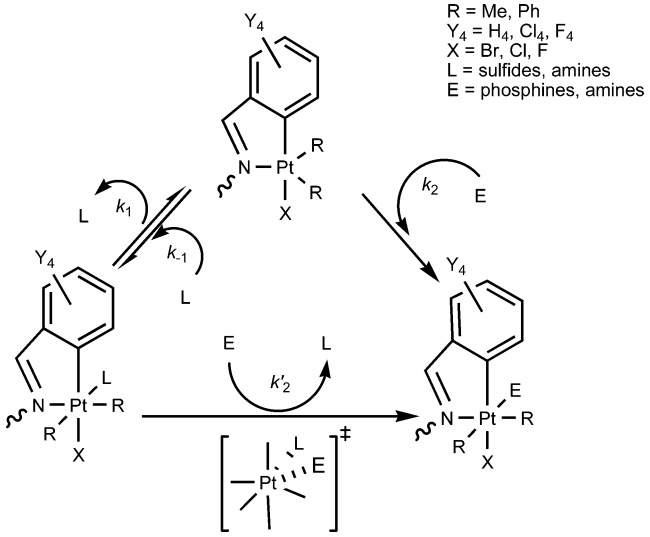

Scheme 2

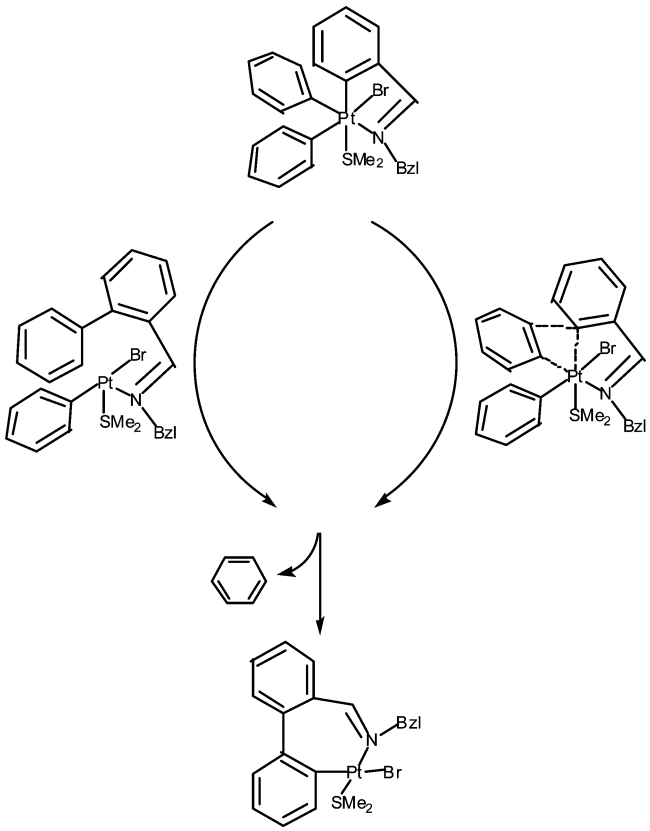

tallic cyclometalated Pt(IV) complexes (Scheme 1).[20] In general, the systems behaved in a dissociatively (k_1, k_{-1}, k_2) activated quasi-labile way.[21,22] The establishment of the first associatively activated substitution reaction on an octahedral Pt(IV) complex (k_2') has been achieved for the R = Me, $Y_4 = F_4$, L = SMe_2, E = $PMePh_2$, $PEtPh_2$, PPh_3 systems.[23]

During the studies of the reaction depicted in Scheme 1 with R = Ph, $Y_4 = H_4$, X = Br, S = SMe_2, the surprising formation of a seven-membered metallacycle via a formal insertion of a phenyl ring in a cyclometalated Pt−C^{aryl} bond has been established. A preliminary communication has already appeared.[24] For the stoichiometric process, two possible pathways could be operative, depending on the reaction either occurring through a real one-step insertion reaction or via a two-step process which involves the reductive elimination of a biphenyl ligand and further cyclometalation reaction, as already proposed for similar systems (Scheme 2).[11,25−27] Despite the fact that dimethyl sulfide dissociation was found to be a key step for the stoichiometric process,[24] no further description of the intimate mechanism has been available. In this paper we present a comprehensive study of the intimate reaction mechanism by which the stoichiometric insertion reaction takes place in these types of systems.

The process has been determined to involve a proper insertion reaction, and the corresponding kinetic, thermal, and baric activation parameters have been measured. Furthermore, the existence of a parallel path, which effectively produces the reductive elimination process of a biphenyl imine ligand, mentioned in the previous communication, has been established. In the latter case no further C−H bond activation has been observed leading to the formation of seven-membered cyclometalated compounds; this fact has also been confirmed by stoichiometric studies. The complete reaction scheme is that indicated in Scheme 3, where the two competitive reaction paths are shown. The kinetic, thermal, and baric activation parameters of the reductive elimination process have also been measured for **Z** = Bzl, Me. The ground-state energies corresponding to the complexes with **Z** = Me appearing in this scheme have also been determined by DFT calculations, justifying the processes observed. Although some calculations had been carried out on nondissociative sp^2-sp^2 reductive elimination reactions on Pt(IV) complexes, as distinct from the equivalent sp^3-sp^3 processes,[28] the possible presence of labile ligands capable of generating a lower coordination number intermediate had not been considered.

The activation parameters corresponding to k_{ins} agree with a substantial enthalpy requirement ($\Delta H^{\ddagger}$ on the order of 100 kJ mol^{-1}). They also involve ordering demands very dependent on both the iminic ligand and the solvent used ($\Delta S^{\ddagger}$ = 64 J K^{-1} mol^{-1} for **Z** = Bzl and 25 J K^{-1} mol^{-1} for **Z** = Me in acetone; $\Delta S^{\ddagger}$ = 64 J K^{-1} mol^{-1} in acetone and −9 J K^{-1} mol^{-1} in chloroform for **Z** = Bzl). Despite this fact, few changes in the volume on going to the transition state ($\Delta V^{\ddagger}$ being ∼0 for all the systems studied) are observed. As for the reductive elimination reactions, k_{red}, they are characterized by values of activation enthalpy and entropy very similar to those already indicated, including an important expansion process on going to the transition state ($\Delta V^{\ddagger}$ in the 10−12 cm^3 mol^{-1} range). For **Z** = Me, the final inserted or reductively eliminated platinum complexes, **6Me** and **5Me**, indicated in Scheme 3, represent an energy gain with respect to the starting compound **1Me**, thus justifying the fine stoichiometric tuning of the processes that favors the formation of the inserted **5Me** complex.

The solution isomerization behavior (as referred to the relative positions of the halide and metalated phenyl ring) of the phosphine-substituted derivative of **5Bzl** has also been fully established, as for other systems of the same family.[29,30] An important tuning of steric origin, capable of overruling the electronic trans effect of the cyclometalated phenyl ring, has been established and a remarkable degree of stereodiscrimination found to be operative. The sequence observed agrees with the possible side products observed in the insertion/reductive elimination full process indicated in Scheme 3.

Results and Discussion

Insertion Reaction. The insertion reaction (**1Z** → **5Z**) indicated in Scheme 3, already stoichiometrically established for **1Bzl**,[24] has been checked and found operative for the

Scheme 3

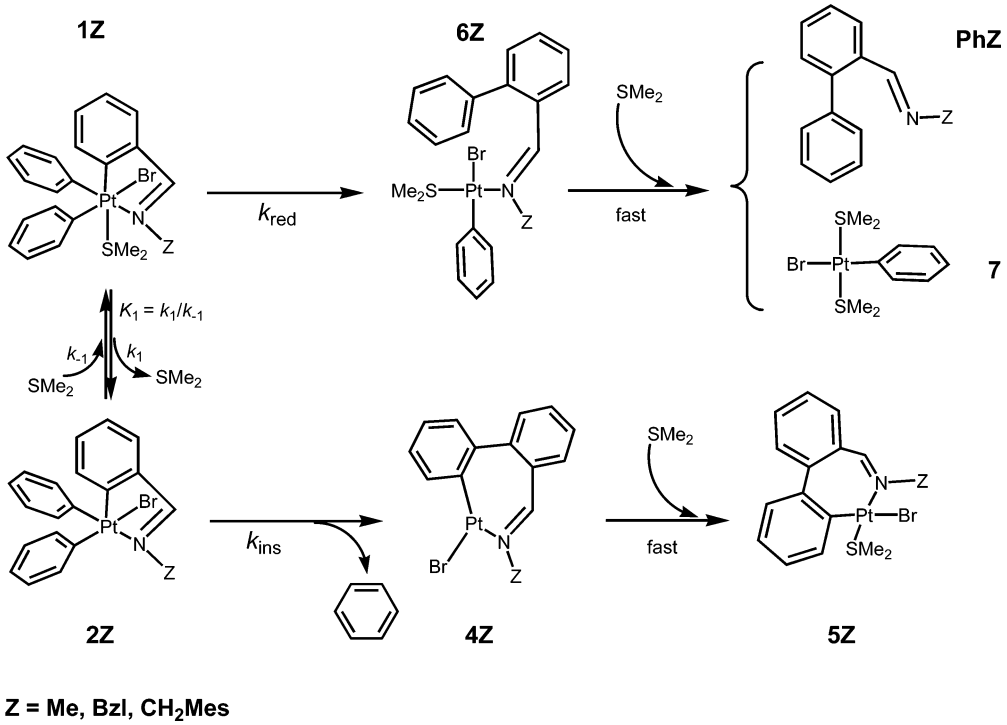

compounds **1Me** and **1CH$_2$Mes**. The isolation of the final **5Z** compounds has not been pursued for these two new compounds; NMR spectroscopy has been found to be a sufficient indicator for the confirmation of processes taking place during the reaction. In our previous studies about the formation of the compound **5Bzl** from **1Bzl**,[24] it was not clear if the reaction proceeded through a simple k_{ins} path (Scheme 3) or through a two-step process involving the reductive elimination reaction (k_{red} path, Scheme 3), followed by a further C−H oxidative addition−reductive elimination of benzene process on the unobserved compound **6Bzl**.[25] In this respect, the reaction of the new diphenylimine 2-(C$_6$H$_5$)C$_6$H$_4$CHNBzl, **PhBzl**, with the compounds [{Pt(Me)$_2$(μ-SMe$_2$)}$_2$], *cis*-[Pt(Ph)$_2$(SMe$_2$)$_2$], and *trans*-[PtBrPh(SMe$_2$)$_2$] (**7**) has been tried in order to establish its reactivity with complexes that could, potentially, produce the desired seven-membered metallacycle observed in the complex **5Bzl**. In all cases the product obtained from these reactions did not correspond to the formation of the seven-membered metallacycle. When the complexes [{Pt(Me)$_2$(μ-SMe$_2$)}$_2$] and *cis*-[Pt(Ph)$_2$(SMe$_2$)$_2$] were used as starting materials, elimination of methane or benzene occurred, respectively, with a simultaneous activation of the C−H bond in the 2′ position of the iminic phenyl ring. That is, the formation of the standard five-membered metallacycle indicated in Chart 1 took place.[5,26,27,31]

Chart 1

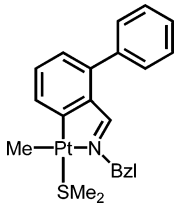

The formation of such five-membered cyclometalated complexes has been demonstrated by the ^{1}H 200 MHz NMR spectrum of the final reaction mixture of the reaction of the diphenyl 2-(C$_6$H$_5$)C$_6$H$_4$CHNBzl imine, **PhBzl**, with the aforementioned starting materials. The spectra showed a set of signals corresponding to a standard five-membered metallacycle: the NC*H* proton appears at 8.64 ppm (J_{PtH} = 57 Hz) or at 8.65 ppm (J_{PtH} = 44 Hz), and the NCH_2 protons appear at 5.13 ppm or at 4.38 and 4.92 ppm (J_{HH} = 12 Hz), for the reaction with [{Pt(Me)$_2$(μ-SMe$_2$)}$_2$] or *cis*-[Pt(Ph)$_2$(SMe$_2$)$_2$], respectively. In both cases the NC*H* signal at 8.79 ppm (J_{PtH} = 122.2 Hz) of the seven-membered metallacycle in **5Bzl** is absent; that is, no C−H bond activation of the distant phenyl ring has taken place. Reaction of the same diphenylimine ligand with *trans*-[PtBrPh(SMe$_2$)$_2$] (**7**) did not produce better results. Under the same reaction conditions, even the coordination of the iminic nitrogen to the Pt(II) center was not observed. Probably the lack of a double statistical reductive elimination process that favors cyclometalation in [{Pt(Me)$_2$(μ-SMe$_2$)}$_2$] or *cis*-[Pt(Ph)$_2$(SMe$_2$)$_2$] prevents the advance of the reaction with such a hindered imine. Furthermore, the presence of only one Pt−C bond in compound

(20) Bernhardt, P. V.; Gallego, C.; Martínez, M.; Parella, T. *Inorg. Chem.* **2002**, *41*, 1747−1754.
(21) Bernhardt, P. V.; Gallego, C.; Martínez, M. *Organometallics* **2000**, *19*, 4862−4869.
(22) Esteban, J.; Font-Bardia, M.; Gallego, C.; González, G.; Martínez, M.; Solans, X. *Inorg. Chim. Acta* **2003**, *351*, 269−277.
(23) Gallego, C.; González, G.; Martínez, M.; Merbach, A. E. *Organometallics* **2004**, *23*, 2434−2438.
(24) Font-Bardía, M.; Gallego, C.; Martínez, M.; Solans, X. *Organometallics* **2002**, *21*, 3305−3307.
(25) Crespo, M.; Font-Bardía, M.; Solans, X. *Organometallics* **2004**, *23*, 1708−1713.
(26) Crespo, M.; Evangelio, E. *J. Organomet. Chem.* **2004**, *689*, 1956−1964.
(27) Crespo, M.; Evangelio, E.; Font-Bardía, M.; Pérez, S.; Solans, X. *Polyhedron* **2003**, *22*, 3363−3369.
(28) Ananikov, V. P.; Musaev, D. G.; Morokuma, K. *J. Am. Chem. Soc.* **2002**, *124*, 2839−2852.
(29) Font-Bardía, M.; Gallego, C.; González, G.; Martínez, M.; Merbach, A. E.; Solans, X. *Dalton Trans.* **2003**, 1106−1113.
(30) Craig, A.; Crespo, M.; Font-Bardia, M.; Klein, A.; Solans, X. *J. Organomet. Chem.* **2000**, *601*, 22−33.
(31) Crespo, M.; Martínez, M.; Sales, J. *Organometallics* **1993**, *12*, 4297−4304.

7 forces the actuation of an associatively activated substitution mechanism[6,32,33] of SMe_2 by **PhBzl**, the full process being very disfavored with the bulky imine ligand. Figure S1 (Supporting Information) collects the ^1H NMR spectral monitoring of the reactivity involved.

It is interesting to note that the cyclometalated Pt(IV) complexes **1Z** are a mixture of the two possible isomers, showing a *mer* (Ph/Ph/SMe_2) and *fac* (Ph/Ph/SMe_2) distribution, the latter being that indicated in Scheme 3 (see the Experimental Section). The *mer*/*fac* isomerization process is found to be slow enough at room temperature to make the two complexes distinguishable by NMR spectroscopy.[24,29] The facile interconversion of the pentacoordinated species formed on sulfide decoordination, **2Z**, can be held responsible for the isomerization process.[34] Theoretical calculations (see Calculations) indicate that the energy demand of the transition state of the *mer* (Ph/Ph/□) $\rightleftarrows$ *fac* (Ph/Ph/□) interconversion process between pentacoordinated species, **2Z**, is low. The free energy value in the gas phase is only 8.72 kJ mol^{-1} for the *mer* to *fac* and 6.09 kJ mol^{-1} for the *fac* to *mer* reactions for the **2Me** complex, thus favoring by 2.63 kJ mol^{-1} the *mer* isomeric form. In view of the existence of these isomeric mixtures and the different substitution labilities already observed for the *mer* (Me/Me/SMe_2) and *fac* (Me/Me/SMe_2) complexes,[29] some experiments on the insertion reaction were carried out in order to determine a possible isomeric discrimination for any of the reactions indicated in Scheme 3. In all cases monitoring of the ^1H NMR spectra during the process did not indicate such discrimination, the *mer* (Ph/Ph/SMe_2) to *fac* (Ph/Ph/SMe_2) isomeric ratio being constant within experimental error during all the processes leading to the final **5Z** complexes.

Reductive Elimination Reaction. Some experiments run at high $[SMe_2]_{added}$ were designed in order to prevent the formation of the expected pentacoordinated species occurring in solution (Scheme 3).[20,21] The results indicated that the insertion reaction from **1Z** to **5Z** complexes is not only considerably retarded but also even totally avoided when high dimethyl sulfide concentrations are used (ca. (200−500) × [Pt]). The same effect was observed whenever the experiments were run at high platinum complex concentration, which has the effect of increasing the presence of non-sulfide dissociated **1Z** complex in the reaction medium. The ^1H NMR monitoring of the aforementioned experiments shows a dominant signal at 2.35 ppm (J_{PtH} = 59 Hz), corresponding to the SMe_2 ligand in *trans*-[PtBr(Ph)-(SMe_2)$_2$] (**7**), while the NC*H* and NCH_2 proton signals showed also the presence of important amounts of free diphenylimine (8.36 and 4.72 ppm for **PhBzl**; see the Experimental Section). The formation of **7** and free diphenylimines, **PhZ**, has to occur via a reductive elimination process of the cyclometalated ligand and of one of the coordinated phenyl groups on hexacoordinated **1Z**, to produce the tetracoordinated **6Z** complexes (Scheme 3). The process is, in fact, fairly similar to that described for similar sp^2-sp^2 reductive coupling in intermediate Pt(IV) complexes detected for some tetraphenylene-generating reactions.[35] The already established preferential coordination of SMe_2 versus the bulky **PhZ** biphenylimines on the Pt(II) complex (see above), plus the stoichiometric excess of SMe_2 in the reaction medium, should then produce compound **7**. Figure S1 also collects the ^1H NMR spectral monitoring of the reactivity involved.

It is interesting to note that the triphenylphosphine derivatives of complexes **1Z** do not undergo such processes on the same time scale. As expected from Scheme 3, the ^{31}P NMR of a solution of **1Bzl** with a 4-fold excess of PPh_3 does not show the presence of any insertion product, **5Bzl**, as indicated by the lack of a signal at 18.7 ppm, corresponding to the opening of the insertion product (see Seven-Membered Ring Opening). Furthermore, after 4 days at room temperature only 5−10% of the initial **1Bzl** complex evolved, via reductive elimination, to *trans*-[PtBrPh(PPh_3)$_2$], as indicated by its ^{31}P NMR signal at 22.8 ppm with J_{PtP} = 3129 Hz. Probably the dramatic differences between the thioether and phosphine ligands account for this fact. Not only is the better donor character of the phosphine ligand bound to disfavor any reductive elimination process from the metal center but also the bulkiness of the ligand induces a more rigid orientation of the phenyl groups, thus disfavoring the highly sterically demanding reductive elimination reaction.

Seven-Membered Ring Opening. Decyclometalation of complex **5Bzl**, via substitutive decoordination of the iminic nitrogen by SMe_2, does not occur on the isolated complex.[24] This lack of reactivity is surprising, given the important trans inductive effect on the iminic nitrogen in the final ligand distribution on the crystallized **5Bzl** complex. The lack of planarity observed in these systems can account for this fact. Nevertheless, during all the insertion processes depicted in Scheme 3 and studied under moderate $[SMe_2]_{added}$ conditions, an extra **Z**-dependent platinum-coupled signal around 2.75−2.85 ppm appears in all cases (2.77 ppm, J_{PtH} = 52 Hz for **Z** = Bzl; 2.86 ppm, J_{PtH} = 52 Hz for **Z** = Me; 2.81 ppm, J_{PtH} = 52 Hz for **Z** = CH_2Mes). The position and coupling of the signal correspond to the existence of a *trans*-[PtBr(*C*-substituted Ph)-(SMe_2)$_2$] type of species.[36] In order to establish the stability of the formed seven-membered metallacycle in **5Z**, the sulfide by triphenyl phosphine substitution has been studied in full detail for the **5Bzl** compound. The process resulted in a rather complicated sequence of changes in the ^{31}P NMR spectra. The speculative series of isomerization reactions involved are depicted in Scheme 4; these are in fact consistent with the structure found for complexes with bulkier DMSO and PPh_3 ligands in seven-membered metallacycle Pt(IV) complexes.[25,37]

When an stoichiometric amount of PPh_3 is added to the complex **5Bzl**, a set of two ^{31}P NMR signals at 16.5 ppm (J_{PtP} = 1832 Hz) and at 15.5 ppm (J_{PtP} = 1888 Hz) appear in the first spectrum recorded. The signals should thus correspond to a coupled isomerization/substitution of the dimethyl sulfide substitution product, as evaluated from the position and platinum coupling of the signal, which indicates a cis (N/P) geometrical distribution.[38] During a period of 30−60 min at room temperature the intensity of the signal at 16.5 ppm diminishes in favor of that at 15.5 ppm, already reported in the synthetic procedure published.[24] The two complexes must have the same basic geometrical arrangement, given the extremely similar magnetic environments of the phosphine. Probably the rigidity of the cyclometalated ring and the bulkiness of the phosphine ligand force the separation of the two possible ring-based isomers, not

(32) Romeo, R.; Plutino, M. R.; Scolaro, L. M.; Stoccoro, S.; Minghetti, G. *Inorg. Chem.* **2000**, *39*, 4749−4755.
(33) Alibrandi, G.; Bruno, G.; Lanza, S.; Minniti, D.; Romeo, R.; Tobe, M. L. *Inorg. Chem.* **1987**, *26*, 185−190.
(34) Wilkins, R. G. *Kinetics and Mechanisms of Reactions of Transition Metal Complexes*; VCH: Weinheim, Germany, 1991.
(35) Edelbach, B. L.; Lachicotte, R. J.; Jones, W. D. *J. Am. Chem. Soc.* **1998**, *120*, 2843−2853.
(36) Hadj-Bagheri, M.; Puddephatt, R. J. *Polyhedron* **1988**, *7*, 2695−2702.
(37) Capapé, A.; Crespo, M.; Granell, J.; Vizcarro, A.; Zafrilla, J.; Font-Bard, M.; Solans, X. *Chem. Commun.* **2006**, 4128−4130.
(38) Crespo, M.; Solans, X.; Font-Bardía, M. *J. Organomet. Chem.* **1996**, 105−113.

Scheme 4

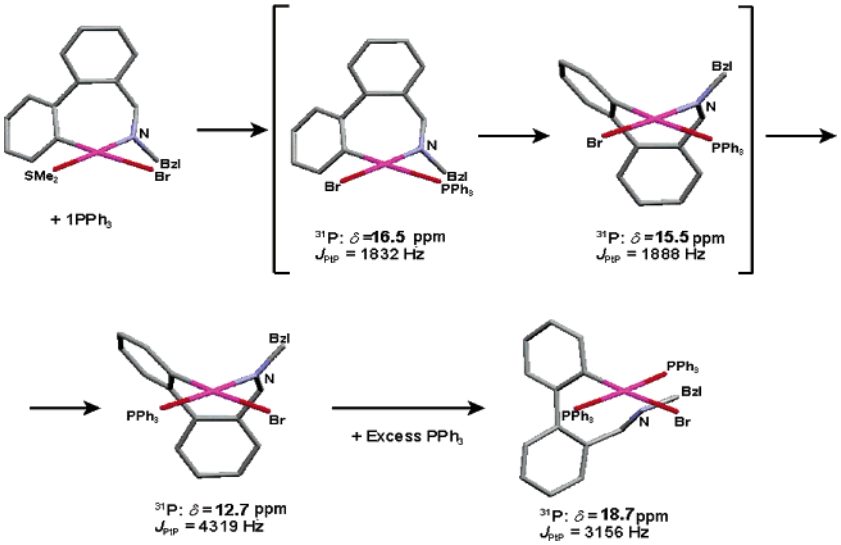

observed in the SMe_2 starting material due to a fluxional conformation movement. In this respect, the hindered rotation or sulfur inversion of the SMe_2 plane in **5Bzl** results in a very wide ^1H NMR signal at room temperature (Figure S1),[29] which prevents a more complete study on other possible fluxional processes taking place simultaneously. During a period of days at room temperature the signal at 15.5 ppm disappears and a new signal at 12.7 ppm (J_{PtP} = 4319 Hz) becomes dominant; the high value of the coupling constant agrees with a trans (N/P) disposition in the complex and the transphobia concept.[25,39,40] If an excess of phosphine is added to the same reaction mixture, another intense signal at 18.7 ppm (J_{PtP} = 3156 Hz) appears. This signal is associated with a decyclometalated *trans*-bis(phosphine) organometallic complex, from comparison with the spectrum of *trans*-[PtBr(Ph)(PPh_3)$_2$] (22.7 ppm (J_{PtP} = 3129 Hz)), obtained from the reaction of PPh_3 with *trans*-[PtBr(Ph)(SMe_2)$_2$] (**7**).

To summarize, the rigidity of the cyclometalated ring and the bulkiness of the PPh_3 ligand enable the NMR observation of the movement between two cycle-based isomeric forms of the diphenylphosphine derivative of **5Bzl**. These evolve finally to the stable cyclometalated complex with the same trans (Br/C) configuration as **5Bzl**. The good Lewis base characteristics of the PPh_3 ligand enable a PPh_3 decyclometalation process, not observed by SMe_2 in **5Bzl**. Although this substitution on the final isolated **5Bzl** is not observed in the presence of large amounts of SMe_2, the intermediate derivatives mentioned above could be tentatively held responsible for the opening of the chelate ring via a Pt−N bond cleavage by SMe_2 in any of them. The signal appearing at ca. 2.75−2.85 ppm can thus be associated with the presence of the putative species *trans*-[PtBr(2-(*C*C_5H_4)-2-C_6H_4CHN**Z**)(SMe_2)$_2$], formed from some transient isomer of **5Bzl** produced on SMe_2 association to the tricoordinated intermediate, **4Z**, in Scheme 3.

Kinetics and Mechanism. (a) Insertion Process. When the monitoring of the insertion reaction from compounds **1Z** to **5Z** (**Z** = Bzl, Me) is carried out at different increasing platinum or added dimethyl sulfide concentrations, an important retardation effect is observed, as already reported.[24] Figure 1a is a clear indication of this behavior; from the inverse plots in Figure 1b it is obvious that the limiting values of k_{obs} at low dimethyl sulfide or platinum complex concentrations are the same within error, which indicates that the rate acceleration due to the decrease of both concentrations has the same basis. Parallel ^1H NMR monitoring of the processes observed indicated that the UV−vis quantified reaction corresponds to the stoichiometric processes indicated in the previous sections.

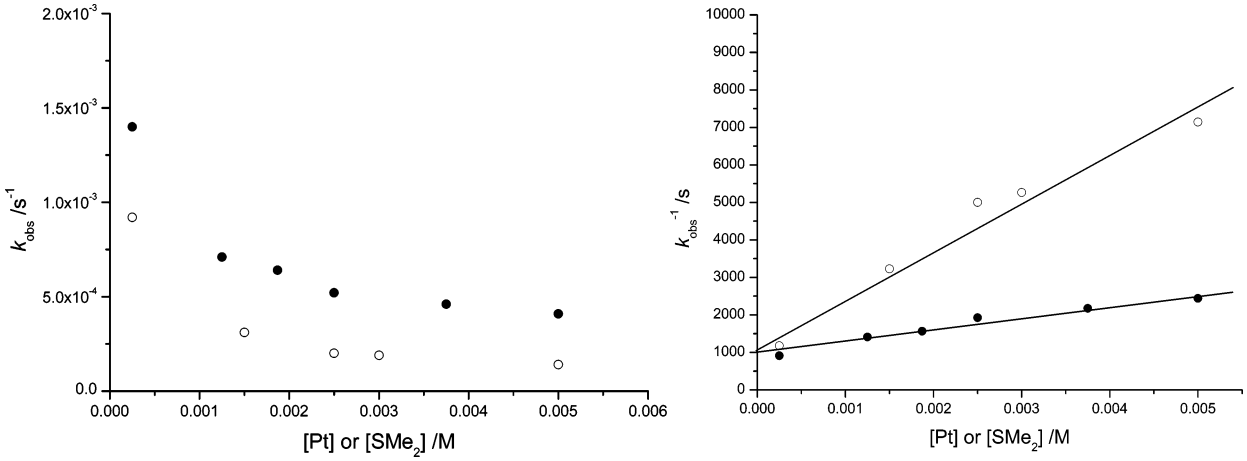

Figure 1. (a, left) Plot of the dependence of the observed rate constant for the insertion reaction for compounds **1Bzl** to produce **5Bzl** on the concentration of (●) platinum complex ($[SMe_2]_{added}$ = 0) or (○) added SMe_2 ([Pt] = 2.0 × 10^{-4} M). (b) Inverse plot of the same dependence. Conditions: acetone solution, 313 K.

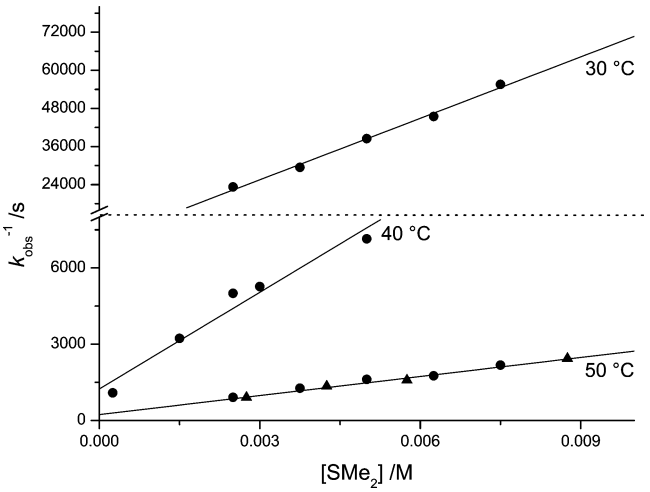

Figure 2. Plot of the dependence of $1/k_{obs}$ on [SMe_2] according to eq 1 for the insertion reaction of compound **1Bzl** in acetone solution at different temperatures and platinum complex concentrations: (▲) [Pt] = 1.25×10^{-4} M; (●) [Pt] = 2.50×10^{-4} M).

Table 1. Kinetic and Thermal and Baric Activation Parameters for the Rate Constants Indicated in Scheme 3

Z	Path	Solvent	^{298}k /s^{-1}	$\Delta H^{\ddagger}$ /kJ mol^{-1}	$\Delta S^{\ddagger}$ /J K^{-1} mol^{-1}	$\Delta V^{\ddagger}$ (T) /cm^3 mol^{-1}(K)
Bzl	k_1[a]	*Acetone*	*0.21*[a]	*60±3*[a]	*−58±1*[a]	*Not measured*
Bzl	k_{ins}	Acetone	7.4×10^{-5}	116±10	64±32	~ 0(318)
	k_{ins}	Chloroform	3.0×10^{-4}	91±7	-9±24	~ 0(308)
	k_{red}	Acetone	2.2×10^{-3}	111±1	73±4	12.0±0.5(290)
	k_{red}	Chloroform	3.6×10^{-3}	96±3	29±10	12.8±0.6(288)
Me	k_{ins}	Acetone	8.9×10^{-5}	104±3	25±10	~ 0(309)
	k_{ins}	Chloroform	7.8×10^{-5}	100±4	10±12	~ 0(313)
	k_{red}	Chloroform	7.3×10^{-4}	94±3	12±9	9.5±1.1(288)

[a] From ref 24.

In this respect, Figure 2 clearly shows that the choice of high platinum complex concentrations is not needed to evaluate the limiting value for k_{obs}, provided $[SMe_2]_{added}$ is kept high enough. Our previous knowledge about substitution reactions on these types of complexes allowed us to relate this behavior with the establishment of a relatively fast dimethyl sulfide dissociation prequilibrium process.[22,29] The dissociation rate constants (k_1), as well as their thermal activation parameters, have already been established for the complex **1Bzl** and are collected in Table 1. According to the reaction mechanism proposed in Scheme 3, eq 1 gives the rate law expected. For the insertion process

$$k_{obs} = \frac{K_1 k_{ins}}{K_1 + [SMe_2]} + \frac{k_{red}[SMe_2]}{K_1 + [SMe_2]}$$

high [SMe_2]: $k_{obs} = k_{red}$

low [SMe_2]: $1/k_{obs} = \frac{[SMe_2]}{K_1 k_{ins}} + 1/k_{ins}$ (1)

occurring at low [SMe_2], the equation is further simplified, as indicated. The values of k_{ins} derived from the plots of $1/k_{obs}$ versus [SMe_2] (Figure 2) are also collected in Table 1. The

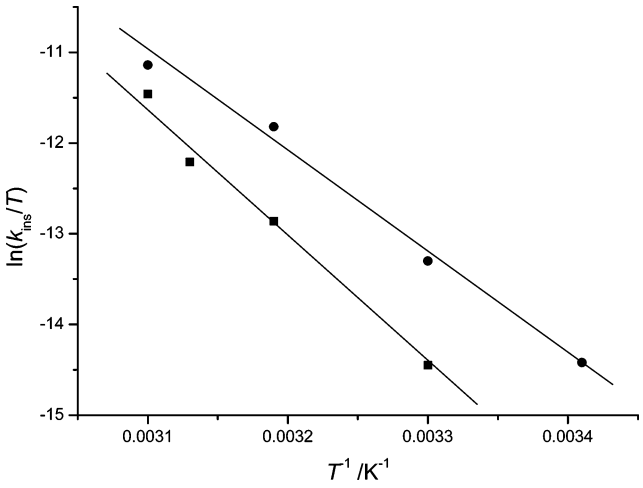

Figure 3. Solvent dependence of the thermal activation parameters for the insertion reaction depicted in Scheme 3 occurring on compound **1Bzl**: (■) acetone solution; (●) chloroform solution.

calculated values for K_1 for the **1Bzl** complex derived from the slope/intercept ratio are in the $(0.6-1.4) \times 10^{-3}$ M range for the systems studied, which, together with the values of k_1, represent a good indication of the fast preequilibrium nature of the SMe_2 dissociation. No further discussion can be carried out, given the high errors involved in the determination.

The platinum concentration dependence of k_{obs} (Figure 1a) also indicates that, as expected, only at relatively high concentrations of platinum complex does the amount of free dimethyl sulfide not increase significantly on decreasing the complex concentration. The good empirical agreement of the values of k_{obs} at platinum concentrations of about $(1-3) \times 10^{-4}$ M, without SMe_2 added, with the values determined for the reciprocal of the intercept in the $1/k_{obs}$ versus [SMe_2] plots (see Figure S2 and Table S1, Supporting Information) enabled us to reduce the amount of kinetic experiment runs. From the temperature and pressure dependence of the value of k_{ins}, the thermal and baric activation parameters associated with the insertion rate constant were determined and are also collected in Table 1. The values agree with a highly enthalpic process taking place, with little compression or expansion to go to the transition state, despite the definite positive (deorganization) value found for $\Delta S^{\ddagger}$ for some of the systems. The differences indicated in Table 1 related to the solvent used, although not large, are evident. Definite differences are observed when **Z** changes from Bzl to Me (Figure 3 collects graphically some of these observations). The trend is the same as that observed for previously studied substitution reactions on these complexes and is related to the higher tendency of the benzylic protons to promote hydrogen bonding with acetone.[20] In this way an increase in dissociation is produced on going to the transition state, where the platinum center has a less acidic character.

The mechanism involved in the process could go through a fully concerted transition state, such as that indicated in Chart 2a, or via the intermediate formation of an hydride complex **3Z**, indicated in Chart 2b, resembling that proposed in the literature as oxidative hydrogen (phenyl, in our case) migration.[41] This hydride complex should rapidly (in a non-rate-determining step) undergo a reductive elimination of benzene to produce the final **5Z** complex, after association with SMe_2. The entropy requirements involving the fully concerted transition state

(39) Cuevas, J. V.; García-Herbosa, G.; Miguel, D.; Muñoz, A. *Inorg. Chem. Commun.* **2002**, *5*, 340−343.
(40) Vicente, J.; Abad, J. A.; Frankland, A.; Ramírez de Arellano, M. C. *Chem. Eur. J.* **1999**, *5*, 3066−3074.
(41) Oxgaard, J.; Muller, R. P.; Goddard, W. A.; Periana, R. A. *J. Am. Chem. Soc.* **2004**, *126*, 352−363.

Chart 2

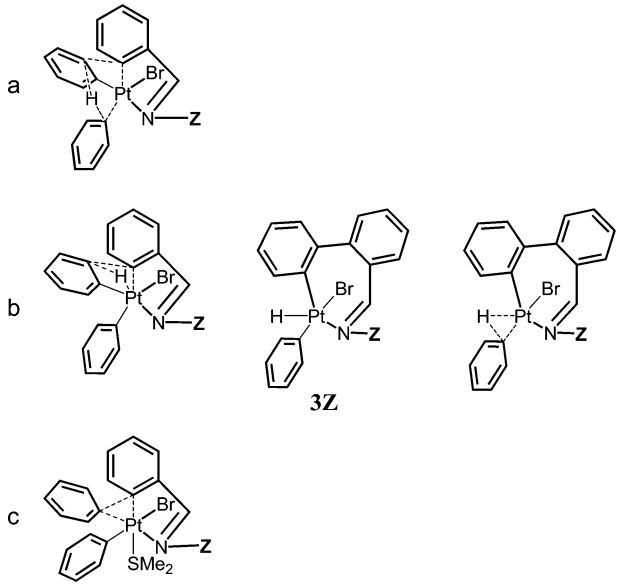

indicated in Chart 2a needing to be highly negative,[42] the known stability of Pt(IV)−H bonds,[2] and the coordinatively unsaturated nature of the **2Z** species prompted us to believe that the process involves the two-step process mentioned above.[41] If, as found for other systems,[17,43] the enthalpy requirement for the formation of the Pt−H bond is much lower than that needed for the R−H reductive elimination, the platinum hydride should exist for a longer period of time at very low temperatures, despite any thermodynamic requirement. Effectively, the cooling of a 1×10^{-4} M sample of **1Bzl** in acetone solution at −70 °C gave a signal at −29.6 ppm in a 300 MHz NMR spectrometer that was tentatively assigned to complex **3Z**, in good agreement with the position of the signals observed for Pt(IV)−H compounds.[44] ^{195}Pt satellites could not be observed, given the extremely low concentration of the hydride (it represents only a small fraction of the complex, the concentration of which is at the 3×10^{-4} M level) and the CSA relaxation expected for compounds containing Pt−H bonds.[45,46] The thermodynamic requirements of the system are made clear by the fact that the signal is lost after longer periods of time, even at low temperature.

The volumes and entropies of activation are expected to have both positive and negative contributions, indicating that the slightly positive ($\Delta S^{\ddagger}$) or zero values ($\Delta V^{\ddagger}$) observed are reasonable. In this respect, the transition state leading to the formation of the putative hydride intermediate, indicated in Chart 2b, should also produce an important differential charge generation responsible for the differences observed when chloroform and acetone are used as solvents. Those are mainly related to activation entropies and are more important for the complexes with the bulkier benzyl-substituted iminic ligand. Nevertheless, the uniformity of the mechanism involved is clear from the $\Delta H^{\ddagger}$ versus $\Delta S^{\ddagger}$ compensation plot, which produces an isokinetic temperature of ca. 60 °C (Figure S3, Supporting Information).

An alternative mechanism could involve the direct reductive elimination of benzene from one of the phenyl ligands and a proton from the other, producing a benzyne ligand Pt^{II} intermediate. Evolution of this complex by insertion of the alkyne into the cyclometalated Pt−C bond is plausible. Nevertheless, the observation of the hydride complex stated before leads us to believe that the existence of the putative benzyne derivative is not probable.

(b) Reductive Elimination Process. The reproducibility of the absorbance versus time traces for the insertion process is very good, but when the added dimethyl sulfide concentration increases considerably, the kinetic profiles show a more complex behavior, with an important induction period and much smaller absorbance changes. When [SMe_2] increases further, the absorbance changes completely invert from those previously observed (Figure 4). Even in some cases, as expected from eq 1, composite diphasic absorbance versus time traces are obtained in experiments run at intermediate [SMe_2], which were consequently avoided for rate measuring. Room-temperature ^{1}H NMR monitoring of the changes occurring at these high SMe_2 concentrations indicated that no insertion process is taking place. Instead, the appearance of compound **7** is taking place via the reductive elimination plus substitution process indicated in Scheme 3 (Figure S1b). The values of k_{obs} determined for these processes, collected in Table S1, clearly indicated that the rate of the process is independent of the concentration of added dimethyl sulfide at the studied platinum complex concentrations. This agrees with the reaction mechanism proposed in Scheme 3 and the very simple rate law $k_{red} = k_{obs}$, obtained from eq 1 at high [SMe_2]. The reductive elimination rate constants and the corresponding thermal and baric activation parameters derived from their temperature and pressure dependence are also collected in Table 1. The process involves both an important expansion (positive $\Delta V^{\ddagger}$) and enthalpic demand to go to the transition state, while $\Delta S^{\ddagger}$ values are small and positive; similar results have been obtained for other reductive elimination processes.[12,17,18,47] The solvent dependence for this process has only been checked for the **Z** = Bzl system. The effect, if existent (Figure S4, Supporting Information), is much smaller than that observed for the insertion processes and only affects activation entropies, which indicates a certain involvement of the acetone solvent in the process. The large errors involved make any deep discussion meaningless. Although these observations are in good agreement with a transition state such as that indicated in Chart 2c, the reductive elimination of the diphenylimine from the hydride complex **3Z**, indicated in Chart 2b, is a plausible alternative for the process. The second possibility can, nevertheless, be disregarded in view of the phenomenology of the SMe_2 dependence of the processes; in the absence of added dimethyl sulfide the reductive elimination process should also be observed, and this is not the case.

Calculations. The complexes involved in the reactions indicated in Scheme 3, shown in Figure 5, have been calculated at the B3LYP/LANL2DZ theoretical level for **Z** = Me. Table S2 collects the energetic parameters obtained in the gas phase, and Cartesian coordinates of the optimized structures are reported in Table S3 (Supporting Information). Given the solvent effect observed in some of the processes studied, we have also conducted single-point calculations on the gas-phase optimized structures obtained, by means of the polarizable continuum model methodology, using chloroform and acetone as solvents. We have not considered direct bonding of discrete solvent

(42) Martínez, M.; Muller, G.; Panyella, D.; Rocamora, M. *Organometallics* **1995**, *14*, 5552−5560.
(43) Wik, B. J.; Lersch, M.; Krivokapic, A.; Tilset, M. *J. Am. Chem. Soc.* **2006**, *128*, 2682−2896.
(44) Wik, B. J.; Lersch, M.; Tilset, M. *J. Am. Chem. Soc.* **2002**, *124*, 12116−12117.
(45) Claridge, T. D. W. *High-resolution NMR Techniques in Organic Chemistry*; Pergamon: Oxford, U.K., 1999.
(46) Ismail, I. M.; Kerrison, S. J. S.; Sadler, P. J. *Polyhedron* **1982**, *1*, 57−59.
(47) Stahl, S. S.; Labinger, J. A.; Bercaw, J. E. *J. Am. Chem. Soc.* **1996**, *118*, 5961−5976.

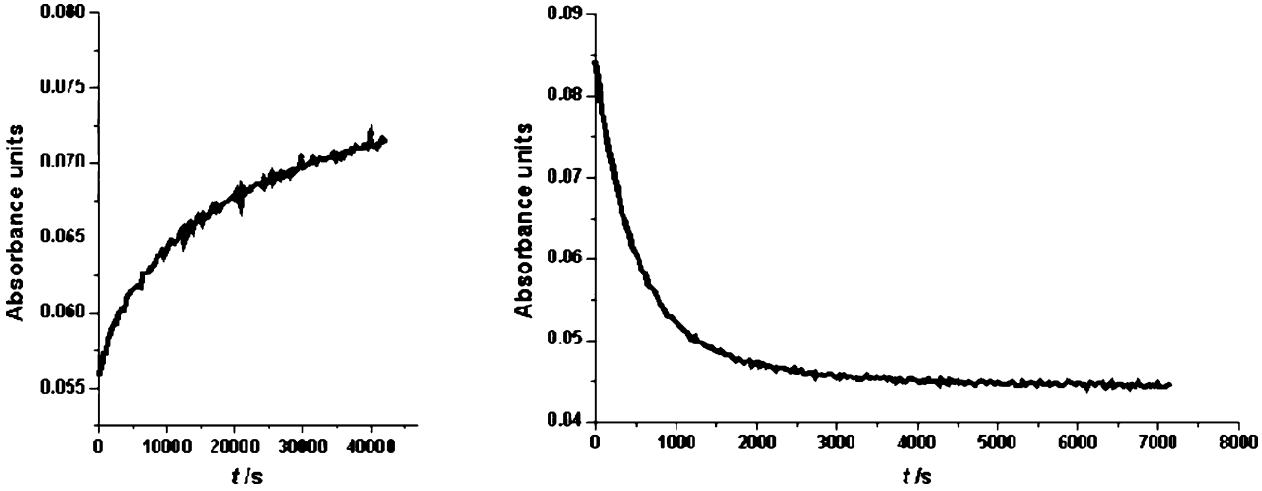

Figure 4. UV−vis spectral changes observed at 370 nm of an acetone solution of compound **1Bzl** with $[SMe_2]_{added} = 0$ M (left, 303 K) or $[SMe_2]_{added} = 2.25 \times 10^{-2}$ M (right, 293 K).

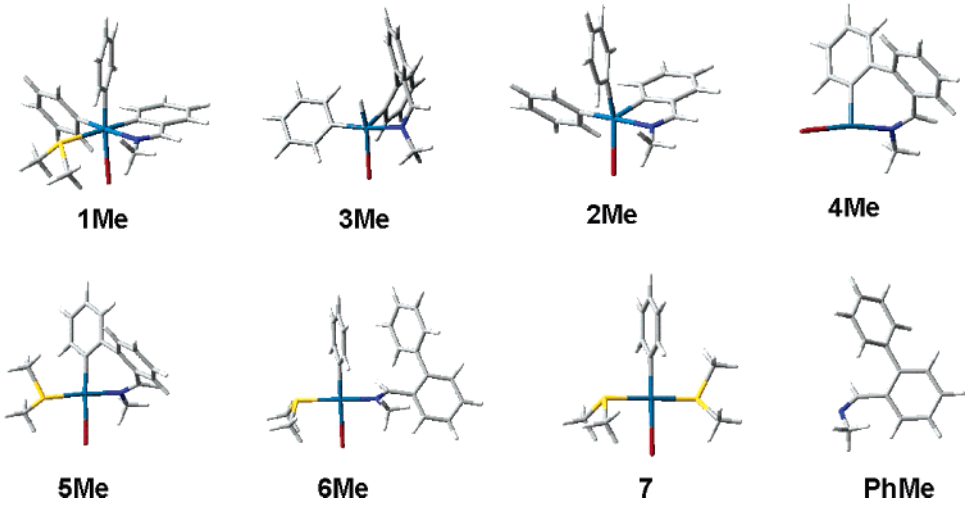

Figure 5. Theoretically calculated structures for the complexes involved in Scheme 3 and Figure 6 (see Table 2).

Table 2. Total Free Energies (*G*) and Relative Free Energies (Δ*G*) in the Gas Phase in Chloroform and in Acetone for the Indicated Structures[a]

	ΔG^b/ kJ mol^{-1}	G^c/hartree (particle)$^{-1}$	ΔG^c/kJ mol^{-1}	G^d/hartree (particle)$^{-1}$	ΔG^d/kJ mol^{-1}
1Me + SMe_2	0	−1139.78	0	−1139.79	0
2Me + 2 SMe_2	−12.17	−1139.76	52.94	−1139.77	47.48
3Me + 2 SMe_2	−0.33	−1139.77	14.11	−1139.76	16.05
4Me + 2 SMe_2 + C_6H_6	−124.24	−1139.79	−33.94	−1139.81	−45.78
5Me + SMe_2 + C_6H_6	−134.60	−1139.82	−92.52	−1139.83	−99.57
6Me + SMe_2	−88.85	−1139.80	−63.05	−1139.82	−64.35
PhMe + **7**	−42.52	−1139.79	−25.71	−1139.80	−28.43
8Me[e] + 2SMe_2	−75.78	−1139.79	−13.85	−1139.80	−24.07
TS2-8 + 2 SMe_2	54.55	−1139.74	114.55	−1139.75	108.83
2Me$_{fac}$ + 2 SMe_2	0	−1139.76	0	−1139.77	0
TS2$_{fac}$−2$_{mer}$ + 2 SMe_2	6.09	−1139.76	2.04	−1139.77	2.67
2Me$_{mer}$ + 2 SMe_2	−2.63	−1139.76	−4.99	−1139.78	−5.26

[a] Extra molecules of SMe_2 an/or C_6H_6 have been added to all structures, except for the seventh entry, in order to properly compare the energies of all entries. [b] Gas phase. [c] Chloroform. [d] Acetone. [e] **8Me** is the species resulting from SMe_2 elimination from **6Me** (see Figure 6).

molecules to a Pt orbital; the theoretical level used and the system size prevents such calculations to be made in a reasonable time. The results are reported in Table 2, where no meaningful differences due to the solvent are detected. Only the consideration of possible hydrogen bonding including discrete solvent molecules in the system is bound to produce extra stabilization of the species and changes between solvents.[48,49]

From these results, it is concluded that the theoretically calculated energetic parameters favor the insertion process (**1Me** → **2Me** → **3Me** → **4Me** → **5Me**; Scheme 3, Figure 6), given the fact that the seven-membered metallacyclic compound **5Me** is the most stable. Hence, under thermodynamically controlled conditions, its formation its predicted to predominate. The reductive elimination process yielding the mixture of products **PhMe** and **7** (**1Me** → **6Me** → **PhMe** + **7**; Scheme 3, Figure 6) will be less favored, as **6Me** is predicted to have a higher stability than the final imine dissociated product. Experimentally, though, **PhBzl** does not react with compound **7**, as indicated before, and complex **7** is the species detected in the final reaction mixture. The need for an associatively activated substitution process to take place in such complexes with only one metal−carbon bond[22] and the bulkiness of the iminic ligands can be easily held responsible for the **7** + **PhMe** lack of reactivity via a prohibitively high energetic transition state for the formation of such a complex. Nevertheless, if the calculations are correct,

(48) Aullón, G.; Bernhardt, P. V.; Bozoglián, F.; Font-Bardía, M.; Macpherson, B. P.; Martínez, M.; Rodriguez, C.; Solans, X. *Inorg. Chem.* **2006**, *45*, 8551−8562.

(49) Reichardt, C. *Solvents and Solvent Effects in Organic Chemistry*; Wiley-VCH: Weinheim, Germany, 2003.

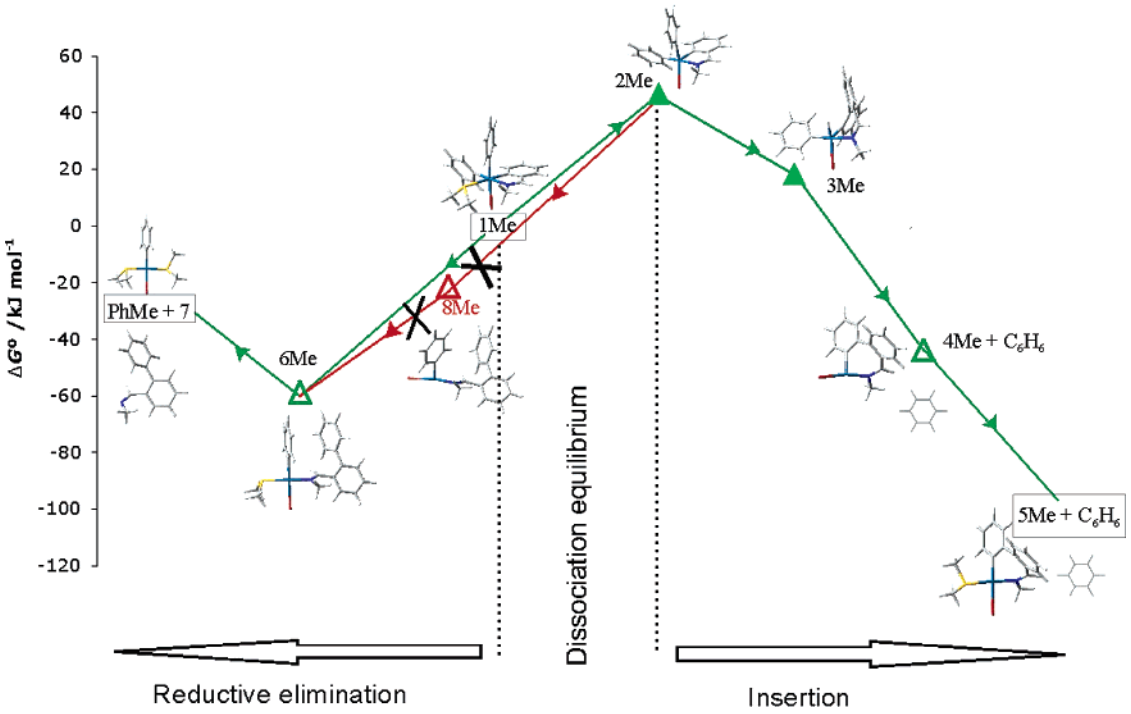

Figure 6. Energetic pathways (green) for the insertion/reductive elimination processes from complex **1Me** in acetone solution. Full points indicate species either kinetically or spectrometrically detected, and empty points refer to calculated-only species. The red line represents the standard path expected for the reductive elimination processes on organometallic Pt(IV) complexes.

complex **6Me** should be the end point of the reductive elimination sequence.

This disagreement between the theoretical results and the experimental observations can be attributed to the weakness of the Pt−S bond compared with the Pt−N bond, as described by the calculations using the double-ς pseudo-orbital basis set LanL2DZ. On going from (**1Me** + SMe_2) to (**2Me** + 2 SMe_2), only a small increase of 55.44 kJ mol^{-1} in the potential energy in the gas phase is obtained, corresponding to the Pt−S bond breaking in **1Me** (Table S2). This demand is largely compensated by the entropic factor that favors the process (ΔG = −12.17 kJ mol^{-1}); in solution this term is less important and the enthalpy dominates the ΔG values in chloroform (+52.94 kJ mol^{-1}) and acetone (+47.48 kJ mol^{-1}) solutions. Furthermore, although the calculated Pt−S bond distance in **5Me** is 2.44 Å, much larger than the experimental value of 2.25 Å determined[24] and close to the values found for similar Pt(IV) systems,[20,21,29] the calculated Pt−N distance is 2.03 Å, very close to the value found in its crystal structure (2.04 Å),[24] confirming the aforementioned fact. As a whole, these discrepancies could be easily related to the π-acid character of the S atom and seem to indicate that the Pt(II) complexes **5Me** and **6Me** could be considerably more stable than the calculations carried out. The effect ought to be even more important for complex **7**, given the fact that two Pt(II)−S bonds are present in this compound. The consequence is that the energy of complexes **5Me**, **6Me**, and **7** indicated in Figure 6 represent a high limit and that the relative values of **6Me** and **7** could be reversed, as observed in the experimental results.

With reference to the insertion process, from **1Me** the formation of **2Me** is not the thermodynamically preferred path, which could make the insertion process difficult in an important way. From **1Me**, the formation of **6Me** is thermodynamically more favorable. From this complex, compound **5Me** can be achieved directly via C−H bond activation to produce a seven-membered-ring Pt(IV) hydride octahedral intermediate followed by benzene elimination (or via its SMe_2-decoordinated analogue, **8Me**, and final reductive elimination of benzene to give **4Me**, after final SMe_2 addition). Complexes **6Z** are not available synthetically from the reaction of **7** and **PhZ**, and seven-membered-ring cyclometalation from the transient **6Z** cannot be ruled out if substitution of imine by sulfide competes in **6Z** complexes with C−H oxidative addition. However, these types of processes have been shown not to take place experimentally; instead, the preferential obtention of five-membered metallacycles occurs (Chart 1).

A simpler alternative path corresponds to a one-step process involving benzene elimination coupled with seven-membered-ring metalation on the hexacoordinate **1Me** complex, with a transition state similar to that indicated in Chart 2a, giving **5Me**. The transition structure (TS1-5) for this path should account for two coupled Pt−C^{aryl} bonds being broken, with a concomitant H migration from a phenyl ligand, that will form part of the final **PhMe**, to the other phenyl ligand that leaves the complex as benzene. A reduction from six- to four-coordination of the platinum center occurs simultaneously with this Pt(IV) to Pt(II) reduction. The complex fine tuning demanded for this TS to take place can preclude its formation, and all attempts made to locate such a delicate TS have been unsuccessful. Furthermore, the stoichiometric $[SMe_2]_{added}$ dependence observed for the overall process and the NMR detection of **3Bzl** agree with the nonviability of this process (see above).

As for the reductive elimination process, the formation of **6Me** from **1Me** occurs through TS1−6 that should describe the cleavage of two Pt−C^{aryl} bonds, the formation of a new C^{aryl}−C^{aryl} bond, plus the reduction from 6 to 4 in the coordination sphere of platinum. However, this transition state is much simpler than the one described in the preceding paragraph and we have not been able to locate it. The equivalent TS involving the SMe_2-dissociated derivatives, **2Me** to **8Me** (TS2-8, Figure S5 and Table 2), has been localized instead, as found for the majority of reductive elimination processes studied on Pt(IV) complexes.[14] From this perspective, it is conceivable that the process **1Me** → **6Me** corresponds, in fact, to a **1Me** → **2Me** →

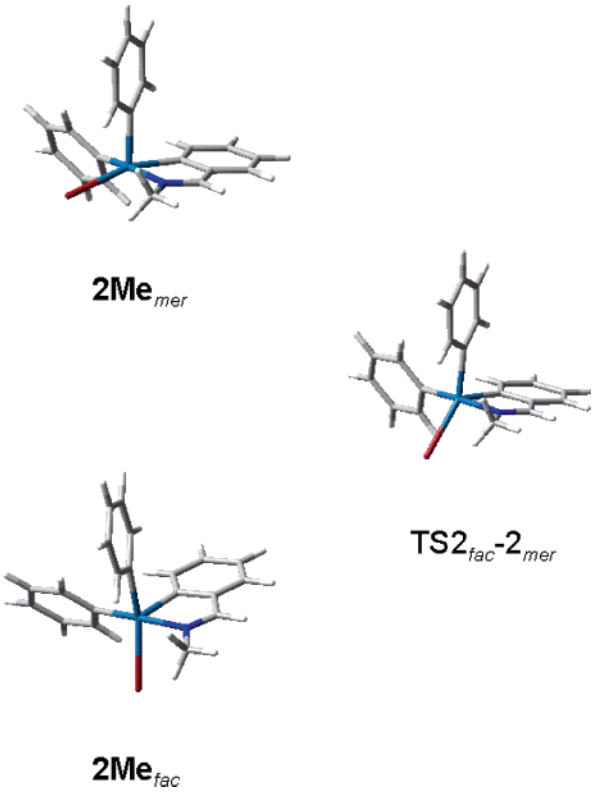

Figure 7. Structures for the *mer* (Ph/Ph/□) ⇄ *fac* (Ph/Ph/□) interconversion process between the **2Me** pentacoordinated species.

8Me → **6Me** path (Figure 6), followed by **6Me** → **PhMe** + **7** to the reductive elimination, competing with **1Me** → **2Me** → **3Me** → **4Me** → **5Me** leading to the insertion process. The stoichiometric and kinetic evidence indicated above do not agree with this sequence; both processes are expected to be slowed down, or even stopped, in with the presence of large amounts of added SMe_2, and this is not the case.

Finally, as indicated before, the transition state of the *mer* (Ph/Ph/□) ⇄ *fac* (Ph/Ph/□) interconversion process between **2Me** pentacoordinated species, expected to be low in energy, has been calculated. This transition structure (TS2$_{fac}$-2$_{mer}$; Figure 7, Table 2) and the results obtained agree, this time very well, with the experimental trend showing the *mer* isomer to be slightly more stable than that having a *fac* conformation.

Conclusions. The disjunctive insertion/reductive elimination process indicated in Scheme 3 and in Figure 6 has been proved from a kinetic, thermodynamic, and stoichiometric study. The reactivity observed is surprising in view of the generally accepted fact that pentacoordinate complexes are needed for reductive elimination reactions on organometallic Pt(IV) compounds. The only reductive elimination processes studied so far occurring on fully octahedral Pt(IV) complexes correspond to C−H and H−H couplings. Some sp^2−sp^2 reductive elimination systems have also been seen to react directly from octahedral complexes; nevertheless, the lack of labile ligands in the coordination sphere of the Pt(IV) center and the laterality of the study do not allow for comparison with ours. Our systems undergo C−C reductive coupling from the hexacoordinate compounds **1Z**, while the parallel insertion reaction takes place from the pentacoordinate intermediates **2Z**. It is clear that important differences in reaction mechanisms can be induced from changes in steric and electronic tuning of the metal center.

For the reactions studied, the C−C coupling observed always takes place between a freely rotating phenyl group and a very rigid phenyl ring of a cyclometalated imine. No diphenyl formation from two freely rotating metalated phenyl rings is detected in the reaction medium; the rigidity of the cyclometalated ring is clearly responsible for this entropic fact. Although DFT calculations pose a reasonable free energy barrier of ca. 110 kJ mol^{-1} for the standard reductive elimination from pentacoordinated **2Z** (middle step in the **1Z** → **2Z** → **8Z** → **6Z** sequence in Figure 6) only that occurring from **1Z** has been observed (**1Z** → **6Z** sequence). There must be a much more favorable energetic balance promoting the **1Z** → **2Z** → **3Z** → **4Z** → **5Z** insertion sequence (Figure 6) from complex **2Z** that is only available in the complexes studied.

In summary, results indicate that the **1Z** → **6Z** reaction path is available with the complexes used, probably due to entropic factors, while the insertion **2Z** → **5Z** reaction path directly competes in these complexes with the **2Z** → **6Z** reductive elimination path, observed in most of the literature reports.

Experimental Section

Instruments. NMR spectra were recorded with a Varian XL-200, a Bruker 250 DRX, and a Varian Unity 300 Plus instrument. Chemical shifts (in ppm) were measured relative to $SiMe_4$ for ^1H and to TMP for ^{31}P; the solvents used were acetone (d_6) or chloroform (d_1). All spectra were obtained in the Unitat de RMN d'Alt Camp de la Universitat de Barcelona at room temperature, unless stated.

Compounds. The noncyclometalated complexes [{Pt(Me)$_2$(μ-SMe$_2$)}$_2$] and *cis*-[Pt(Ph)$_2$(SMe$_2$)$_2$] have been prepared according to the published procedures;[50,51] their ^1H NMR characterization agreed with the values previously reported. The complex *trans*-[PtBr(Ph)(SMe$_2$)$_2$] has been prepared from *trans*-[Pt(Br)$_2$(SMe$_2$)$_2$] according to the standard procedure involving reaction with LiPh. The values found for its proton NMR spectrum (2.35 ppm, J_{PtH} = 59 Hz) are very similar to those indicated[36] for the analogous *trans*-[PtCl(Ph)(SMe$_2$)$_2$] and agree with the expected for its formulation; therefore, further characterization was not pursued.

The 2-BrC_6H_4CHN**Z** imines used in this study have been prepared according to the standard aldehyde plus amine condensation reaction widely applied.[52] For **Z** = Bzl the proton NMR spectrum agrees with that published, while for **Z** = Me and **Z** = CH_2Mes the new imines have proton NMR spectra that agree with the expected formulation: δ 3.59 [3H], 8.66 [1H] ppm for **Z** = Me and δ 2.29 [3H], 2.44 [6H], 4.91 [2H], 8.75 [1H] ppm for **Z** = CH_2Mes. The new 2-(C_6H_5)C_6H_4CHNBzl imine **PhBzl** has been prepared by the same procedure from 2-(C_6H_5)C_6H_4COH and H_2-NBzl: δ 4.72 [2H], 8.36 [1H] ppm.

The cyclometalated complexes **1Bzl**, **1Me**, and **1CH$_2$Mes** have been prepared by oxidative addition of the C−Br bond of the corresponding 2-BrC_6H_4CHN**Z** imines to the *cis*-[Pt(Ph)$_2$(SMe$_2$)$_2$] complex.[21,24,25] Their ^1H NMR spectra agree with the formulation expected (Table S4); in all cases the proton NMR spectra of the complexes indicated the coexistence of *mer* (Ph/Ph/SMe$_2$) and *fac* (Ph/Ph/SMe$_2$) isomeric forms of the compounds in the reaction mixture.[20,29] No elemental analyses were carried out on these complexes, given their high reactivity to produce immediate parallel insertion and reductive elimination reactions, which prevented the existence of a 100% pure sample of the dimethyl sulfide derivatives. Nevertheless, the substituted triphenylphosphine derivative of **1Bzl** has already been described and its X-ray crystal structure determined.[24]

(50) Scott, J. D.; Puddephatt, R. J. *Organometallics* **1983**, *2*, 1643−1648.
(51) Rashidi, M.; Fakhroeian, Z.; Puddephatt, R. J. *J. Organomet. Chem.* **1991**, *406*, 261−267.
(52) Gómez, M.; Granell, J.; Martínez, M. *Inorg. Chem. Commun.* **2002**, *5*, 67−70.

The seven-membered cyclometalated inserted complex **5Bzl** has already been fully characterized and described.[24] The corresponding **5Me** and **5CH$_2$Mes** complexes have been prepared by the same method, and their ^{1}H NMR spectra (Table S4) show the distinctive resonance of the NC*H* proton around 8 ppm with a very large J_{PtH} value of about 120 Hz. No further characterization was pursued, given the simultaneous presence in the reaction medium of the free **PhZ** imine, *trans*-[PtBr(Ph)(SMe$_2$)$_2$], and the putative *trans*-[PtBr-(2-(*C*C$_5$H$_4$)2-C$_6$H$_4$CHN**Z**)(SMe$_2$)$_2$] complexes (see Results and Discussion).

Kinetics. The reactions were followed for the **1Bzl** and **1Me** complexes by UV−vis spectroscopy in the 500−330 nm range, where none of the solvents absorb. Atmospheric pressure runs were recorded on an HP8452A or Cary50 instrument equipped with a thermostated multicell transport. Observed rate constants were derived from absorbance versus time traces at the wavelengths where a maximum increase and/or decrease of absorbance was observed. For runs at variable pressure, a previously described pressurizing system and pillbox cell was used;[53] the system was connected to a J&M TIDAS spectrophotometer, which was used for the absorbance measurements. No dependence of the values of the observed rate constants on the selected wavelengths was detected, as expected for reactions where a good retention of isosbestic points is observed. The general kinetic technique is that previously described.[4,20,24] When SMe$_2$ was added to the reaction mixture, pseudo-first-order conditions were maintained; but in some cases (see Results and Discussion) no dimethyl sulfide was added to the reaction mixture. The platinum complex concentration was maintained at a minimum of 2.5×10^{-4} M (unless stated) to avoid undesired decomposition reactions and platinum complex rate dependence, both caused by the preequilibrium dissociative reaction described.[21] Table S1 collects all the obtained k_{obs} values for all the systems studied as a function of the starting complex, process studied, platinum and dimethyl sulfide concentrations, solvent, pressure, and temperature. All post-run fittings were carried out by the standard available commercial programs.

Calculations. The theoretical study has been conducted with the Becke hybrid density functional (B3LYP)[54,55] method as implemented in the Gaussian03 program.[56] The double-ς pseudo-orbital basis set LanL2DZ, in which Pt, S, and P atoms are represented by the relativistic core LanL2 potential of Los Alamos,[57] was used. Solvent effects were taken into account by means of polarized continuum model calculations[58,59] using standard options. The energies of solvation were computed in chloroform ($\epsilon = 4.9$) and acetone ($\epsilon = 20.7$) at the geometries optimized in the gas phase.

Acknowledgment. We acknowledge financial support of the CTQ2006-14909-C02-02/BQU and BQU2003-04168-C03-03 projects from the Ministerio de Educación y Ciencia and the Fundació Bancaixa-UJI (project P1-1B2005-15). We also thank the *Servei d'Informàtica* and the *Departament de Ciències Experimentals* of the Universitat Jaume I for computer facilities.

Supporting Information Available: Table S1, giving the observed rate constants for the systems studied as a function of starting material, SMe$_2$ concentration, solvent, temperature, and pressure, Table S2, giving energies calculated at the B3LYP/LANL2DZ level in the gas phase for the compounds studied, Table S3, giving Cartesian coordinates for all the optimized structures of the species involved in this work, Table S4, giving ^{1}H NMR data for all of the new complexes prepared, Figure S1, showing changes occurring in the SMe$_2$ signal zone of the ^{1}H NMR spectra for the reaction of **1Bzl**, Figure S2, giving a plot of the dependence of $1/k_{obs}$ on [SMe$_2$] for the insertion reaction of compound **1Bzl**, Figure S3, giving a $\Delta H^{\ddagger}$ versus $\Delta S^{\ddagger}$ compensation plot, Figure S4, showing the solvent dependence of the thermal activation parameters for the reductive elimination occurring on compound **1Bzl**, and Figure S5, showing the theoretically calculated structure for the complex **8Me** and for TS2-8. This material is available free of charge via the Internet at http://pubs.acs.org.

OM060818E

(53) Gómez, M.; Granell, J.; Martínez, M. *Organometallics* **1997**, *16*, 2539−2546.

(54) Lee, C.; Yang, W.; Parr, R. G. *Phys. Rev. B* **1988**, *37*, 785−789.

(55) Becke, A. D. *J. Chem. Phys.* **1993**, *98*, 5648−5652.

(56) Frisch, M. J.; et al. *Gaussian03*, Revision C.02; Gaussian Inc., Wallingford, CT, 2004.

(57) Hay, P. J.; Wadt, W. R. *J. Chem. Phys.* **1985**, *82*, 270−273.

(58) Tomasi, J.; Persico, M. *Chem. Rev.* **1994**, *94*, 2027−2094.

(59) Amovilla, C.; Barone, V.; Cammi, R.; Cancès, E.; Cossi, M.; Mennucci, B.; Pomelli, C. S.; Tomasi, J. *Adv. Quantum Chem.* **1998**, *32*, 227−261.